ELSEVIER

Journal of Chromatography A, 913 (2001) 221–231

JOURNAL OF CHROMATOGRAPHY A

www.elsevier.com/locate/chroma

Validation of a chromatography data analysis software

Attila Felinger[a], Georges Guiochon[b,c,*]

[a]*Department of Analytical Chemistry, University of Veszprém, Egyetem u. 10, Veszprém, H-8200 Hungary*
[b]*University of Tennessee, Department of Chemistry, Knoxville, TN 37996-1600, USA*
[c]*Division of Chemical and Analytical Sciences, Oak Ridge National Laboratory, Oak Ridge, TN 37831-6120, USA*

Abstract

The performance of chromatography data analysis software packages is of cardinal importance when the precision and the accuracy of a chromatographic system are evaluated. Users cannot rely on a procedure generating chromatographic data of known accuracy. Holistic approaches cannot always be entirely trusted. We propose a new method consisting in validating a data analysis package against computer generated chromatograms of exactly known characteristics by feeding these chromatograms into the vendor supplied software and comparing the results supplied by the software and the exact answers. We simulated symmetrical and tailing chromatograms and processed these signals with the Agilent Technologies (formerly Hewlett-Packard) ChemStation software. The noise profile (i.e. the power spectrum of the baseline) was determined for a HPLC UV detector prior to the calculations, and chromatograms of different signal-to-noise ratios were used for the analysis. For every chromatogram, we simulated 25 replicates with identical signal-to-noise ratios but different noise sequences. In this manner, both the random and the systematic errors of the retention data and peak shape characteristics can be evaluated. When analyzing tailing peaks, we simulated the effects of extra-column band broadening and those of column overload. Our calculations show that the general performance of the data analysis system studied is excellent. The contribution of the random error originating from the data analysis procedure is in most cases negligible compared to the repeatability of the chromatographic measurement itself.

Keywords: Validation; Data analysis software

1. Introduction

The correct evaluation of the actual accuracy and precision of analytical measurements assumes an increasing importance with the current trends of the validation and quality control issues. The holistic validation of an analytical procedure requires that every part of the applied analytical technique be validated, including the instrument, its computer hardware and its software. Although suitable software validation should be provided by the vendor, we have read more statements to the effect that the software being a series of logical statements and deductions, should achieve what it purports to do, than data effectively demonstrating the validity of this assertion. It seems to be essential nowadays that users be able to check and verify, when needed, the performance of the software that they use. However, by contrast with a balance that can be validated by weighing masses of accurately known weight, chromatograms cannot be validated by feeding accurately known chromatographic data directly to the software. Data of sufficient accuracy cannot be generated by HPLC. A recent thorough and rigorous study of the repeatability of reversed-phase liquid chromatographic measurements [1–4] revealed that the re-

*Corresponding author. Tel.: +1-856-974-0733; fax: +1-856-974-2667.

E-mail address: guiochon@utk.edu (G. Guiochon).

0021-9673/01/$ – see front matter
PII: S0021-9673(00)00979-1

peatability of retention times was below 0.05% for most compounds and the repeatability of the plate numbers was between 1 and 2.5%. The accuracy of these data remains unknown, however. One may rightfully expect that, even at this precision level, the software itself has no traceable impact on the precision of the chromatographic measurements.

The ultimate precision of the data analysis software must be evaluated accordingly. The direct validation of a chromatographic integrator using highly accurate signals fed into the integrator unit through a hardware unit that translated synthetic, computer generated symmetrical and tailing peaks into an electrical signal that the integrator could process was reported by Dyson [5]. The hardware unit acted as an interface between the computer and the integrator. Engelhardt and Siffrin [6] proposed means of validation of HPLC systems and components but did not mention the software itself. Although it does not seem that a comparable study was performed in HPLC, Faller and Engelhardt recently compared the performance of commercial software packages for the integration of capillary electropherograms [7]. They found that when the signal-to-noise ratio is above 35, all packages give a precision better than 1% for the peak area.

We propose to validate the instrument software directly, by feeding chromatograms of known characteristics to the software programs, comparing the results obtained with the parameters of these chromatograms, and testing the precision and accuracy of the various modules of the software performing peak integration, retention time and peak efficiency determinations, and other parameter calculations. A similar approach was used in the past, in gas chromatography [8,9]. Most HPLC instruments now use a powerful microcomputer as the data station. This computer is able to generate the synthetic chromatograms needed, calculating them by using any of different peak shape models. Unfortunately, vendors do not convey up front any information to users about how to calculate synthetic chromatograms that could be processed by the vendor supplied software. Data formats and integration routines used by some vendors are not patented but considered as confidential. However, Agilent Technologies (Palo Alto, CA, USA) data file formats are available upon completion of a confidentiality disclosure agreement. We availed ourselves of this facility in the present work.

2. Theory

2.1. The baseline noise

Most conveniently, noise can be analyzed by calculating the power spectrum of the noise sequence, because the plot of the logarithm of the power spectrum against the logarithm of the frequency reveals the major characteristics of the noise. Several studies have examined the noise in chromatographic systems. The baseline in most of the systems examined exhibited flicker noise [10,11]. Hayashi and Matsuda [12] approximated the noise of the chromatographic baseline with the combination of two independent random processes: a white noise and a Markov process. The blend of these two stochastic processes yields a random sequence whose properties resemble those of the flicker noise for a wide frequency range. The Markov process is one of those used to describe the random variable r at a given time based on its value at a previous observation. This assumes that there is a correlation between the previous and the current value of the random variable. The Markov process is formulated as

$$r(t + \Delta t) = \rho r(t) + m(t) \tag{1}$$

where $r(t + \Delta t)$ is the value of the random variable r at time $t + \Delta t$, ρ is a correlation coefficient indicating the probability of retaining the previous value of r, and $m(t)$ is a white noise sequence.

The autocorrelation function of the Markov process is

$$C(t) = \frac{\sigma_m^2}{1-\rho^2} \cdot \exp\left(- \frac{(1-\rho)\, t}{\Delta t} \right) = C_0\, \mathrm{e}^{-\alpha t} \tag{2}$$

where $C_0 = \sigma_m^2/(1-\rho^2)$ and $\alpha = (1-\rho)/\Delta t$. The power spectrum of the Markov process is the Fourier transform of the above autocorrelation function:

$$P_r(\omega) = C_0 \cdot \frac{2\,\alpha}{\alpha^2 + \omega^2} \tag{3}$$

The random chromatographic baseline is considered

as the sum of the above Markov process and an independent white noise:

$$x(t) = r(t) + w(t) \tag{4}$$

The power spectrum of the white noise is a horizontal line whose position is determined by its variance, $P_w(\omega) = \sigma_w^2$. The power spectrum of the combined stochastic process can be summed from those of the individual processes, for they are independent:

$$P(\omega) = C_0 \cdot \frac{2\,\alpha}{\alpha^2 + \omega^2} + \sigma_w^2 \tag{5}$$

Parameters C_0, α, and σ_w can be determined by fitting the above model to the power spectrum of the measured baseline.

2.2. The chromatographic peak shapes

In this study we used the three peak shape models that are fundamental in chromatography. These are the Gaussian peak, the exponentially convoluted Gaussian peak and the langmuirian overloaded peak profiles.

In linear, analytical chromatography, all models predict a peak shape that is indistinguishable from the Gaussian peak at the nowadays standard column efficiencies [13]. When using Gaussian peak shapes to verify the chromatography data analysis software, many of the attributes can be calculated analytically from the parameters used to generate the chromatogram. When the peak shape model is written as

$$f(t) = h_0 \exp\left[-\frac{(t - t_R)^2}{2\,\sigma^2} \right] \tag{6}$$

the peak area is $A = h_0\sigma\sqrt{2\pi}$, the peak width at any fractional peak height ($r = h/h_0$) is $w_r = 2\sigma\sqrt{-2\ln r}$. Furthermore the number of theoretical plates is expressed as $N = (t_R/\sigma)^2$.

In analytical chromatography, peak tailing is generally attributed to occasional column overload, heterogeneity of the packing bed, heterogeneous sorption kinetics, or extra-column effects. For the purposes of this study we selected two kinds of tailing peaks: (i) the profile given for a pulse injection by the exponentially modified Gaussian (EMG) model, a model that accounts for mixer-type extra-column effects; and (ii) the profile calculated for an overloaded column using the equilibrium–dispersive model of nonlinear chromatography and assuming Langmuir isotherm.

The EMG peak shape can be calculated as the convolution of a Gaussian peak with an exponential decay function:

$$f(t) = \frac{A}{2\tau} \cdot \exp\left(\frac{\sigma^2}{2\,\tau^2} - \frac{t - t_R}{\tau} \right) \times \left[1 - \mathrm{erf}\left(\frac{\sigma}{\sqrt{2}\,\tau} - \frac{t - t_R}{\sqrt{2}\,\sigma} \right) \right] \tag{7}$$

where t_R and σ are the retention time and standard deviation of the Gaussian peak, respectively; whereas τ is the time constant of the exponential decay function. The peak height, the location of the peak maxima, the peak width at any height can only be calculated numerically for the EMG peak. The moments, however, are readily available. The first moment is $\mu_1 = t_R + \tau$, the second central moment is $\mu_2' = \sigma^2 + \tau^2$. Therefore, the moment-based statistical plate number is $N = (t_R + \tau)^2/(\sigma^2 + \tau^2)$. The skew and the excess can also be calculated analytically, but the other parameters must be determined by numerical calculation.

For the nonlinear model, the band profile can be calculated numerically only. The finite difference method can be used for the integration of the mass balance equation [13] and the peak attributes can be evaluated numerically.

3. Computations

Chromatograms were generated by combining a noisy baseline and a synthetic peak, both obtained by the appropriate software subroutines. All chromatograms were generated 25 times successively, with identical peak shape parameters and signal-to-noise ratios, but with different noise sequences. All programs were written in the Fortran language and run on Unix workstations of the University of Tennessee Computing Center. The data files were downloaded to a personal computer and translated to binary files using a text file conversion utility provided by the Agilent Technologies (formerly, Hewlett-Packard, Little Falls Analytical Division). The chromatograms then were processed using the ChemStation Rev.

A.05.01 software. The peak area, peak height, retention time, peak width, number of theoretical plates, and USP tailing factor were determined for every chromatogram. The average values and the standard deviation of the parameters estimated by the data station using the synthetic chromatograms submitted were calculated in order to evaluate the accuracy and the precision of the calculations.

Symmetrical and asymmetrical peaks were generated by means of the above peak shape models and the level of noise was changed so that the signal-to-ratio be between 10 and 10000. The signal-to-noise ratio was calculated as $S/N = h/(4\sigma_N)$ where σ_N is the standard deviation of the baseline noise sequence [14].

4. Results and discussion

4.1. Baseline noise analysis

In order to properly model noisy chromatograms, the noise pattern of the baseline was first investigated. For that purpose, the signal of an Agilent Technologies HP 1100 liquid chromatograph, equipped with a diode array detector, was used. Baselines were recorded at a frequency of 20 Hz by pumping mobile phase. The measurement of the baseline was repeated 25 times and the power spectra of these baseline samples were averaged. The averaged power spectrum is plotted in Fig. 1a. The noise profile can be characterized with the power spectrum of $P(f) \sim f^{-1.66}$ (see the dotted line in Fig. 1a), for frequencies below 1 Hz. This noise structure is a transition between the flicker noise and the brown noise. The high frequency noise is magnified in Fig. 1b on a linear scale. This section of the power spectrum shows the constant pattern of the white noise and several spikes, most of them approximately 0.5 Hz apart. The spikes in the power spectrum of the noise can be attributed to the operation of the pump heads [15].

The combined power spectrum (see Eq. 5) was fitted to the average power spectrum of the baseline. The following numerical parameters were obtained: $C_0 = 1.505 \cdot 10^{-6}$, $\alpha = 1.971 \cdot 10^{-3}$, and $\sigma_w = 3.114 \cdot 10^{-4}$. This model (dashed line in Fig. 1a) approximates the measured power spectrum fairly well in the whole frequency range. Therefore, we used Eq. 5 with the above numerical values to generate the chromatographic baseline. The average of 25 synthetic baseline noise sequences is plotted

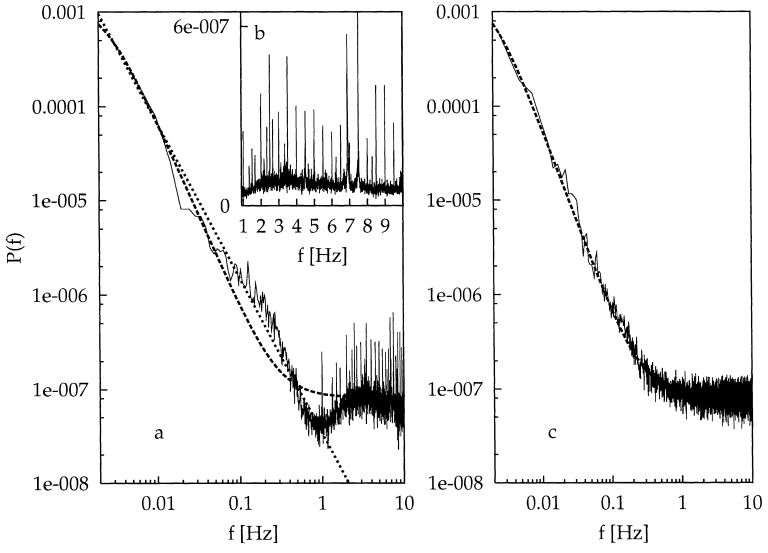

Fig. 1. (a) Log–log plot of the power spectrum of the baseline noise. The measured noise (solid line), the exponent noise model (dotted line), the combined noise model given in Eq. 5 (dashed line); (b) Linear plot of the high frequency noise; (c) Log–log plot of the generated noise (solid line) and the combined noise model (dashed line).

(solid line) in Fig. 1c together with the combined model (dashed line). One can see that the synthetic noise resembles quite well the original baseline noise except for the spikes observed at high frequencies. The effect of the spikes on the noise can be neglected, however, because the intensity of the spikes is smaller by several orders of magnitude than the low frequency elements of the noise.

The two power spectra plotted in Fig. 1 are based on the noisy baselines as output by the Chemstation. Therefore, both the experimentally observed and the simulated noise sequences are affected by the same quantization error of the digital signal processing, so the power spectra in Fig. 1a,b are directly comparable. Although the original detector noise is altered by the digitalization process, this effect is marginal. The only major effect of the quantization process on a signal is that the variance of the signal is increased by $q^2/12$ where q is the quantization level [14]. So, the effect of quantization on the noise results in an approximately 3% (at $S/N = 10\,000$) and 0.3% (at $S/N = 3000$) increase of the noise variance in the case of the two smoothest chromatograms we generated. For the rest of the chromatograms, this effect is completely negligible.

4.2. Preliminary calculations

The heights of the generated peaks were close to the maximum capacity of the software in order to reduce the discretization error to a negligible contribution [14]. The integration of noise-free symmetrical peaks was tested first, using a Gaussian peak with a retention time $t_R = 100$ s and a standard deviation $\sigma = 1.25$ s. With these values, the plate number is $N = 6400$, a typical value for the peak of an early eluting component on a fairly efficient column. In this set of calculations, the data acquisition frequency was 20 Hz, thus giving 25 points per σ which is more than recommended by some researchers [16,17]. The location of the Gaussian peak was shifted from the original $t_R = 100$ s position to $t_R + \sigma$ in 25 steps, leaving all the other parameters unaffected.

The calculations of the peak area, peak height, and retention time were not sensitive to these minor changes of the location of the peak. However, the measured peak width and, accordingly, the number of theoretical plates showed a peculiar correlation with the peak location. The ChemStation offers a choice of four different means of measurement of the peak width: (i) at half height; (ii) at 5% of the peak height (where the USP tailing factor is determined); (iii) at 4.39% of the peak height (where the width of a Gaussian peak is 5σ); and (iv) by drawing the tangents to the inflection points [18]. The number of theoretical plates is also derived in four different manners, from (i) the width at the peak at half-height; (ii) the 5σ width of the peak; (iii) the tangent peak width; and (iv) the first and second statistical moments of the peak.

The different peak width values determined by the ChemStation are plotted in Fig. 2. First of all, there is a slight systematic error in the peak width measurement, approximately 0.63% at half height, 0.31% at 5% of the peak height, 0.4% at 5σ width, and on average 0.43% at the tangent peak width. The above reported relative deviations correspond approximately to one half of the data acquisition time.

It is surprising to see that the peak widths obtained at half-height and at 5% of the peak height oscillate between two different values, with a constant frequency, whereas the values obtained at 4.39% of the peak height remain constant, and those derived from the position of the inflection tangent increased periodically. These phenomena are probably due to the fact the ChemStation software does not interpolate properly when the different width values are evaluated. A least-squares fitting of the data to a parabola would probably enhance the accuracy of the peak width. Since the number of theoretical plates is calculated from the peak width, this error is carried on and causes a minor bias in the reported plate number values (see later). This result confirms that a peak should contain several hundreds of digitized points for accurate peak width and column efficiency measurements [16,17,19].

Another unusual feature of the integration is that the software consequently reports a different value for the peak area and for the 0th moment (μ_0). The difference is minor for noise-free peaks (around 0.004%) but it increases continuously with increasing noise level. These two values should be identical by definition. Most probably, the moments are calculated by a different subroutine of the software and the integration limits are different for the simple

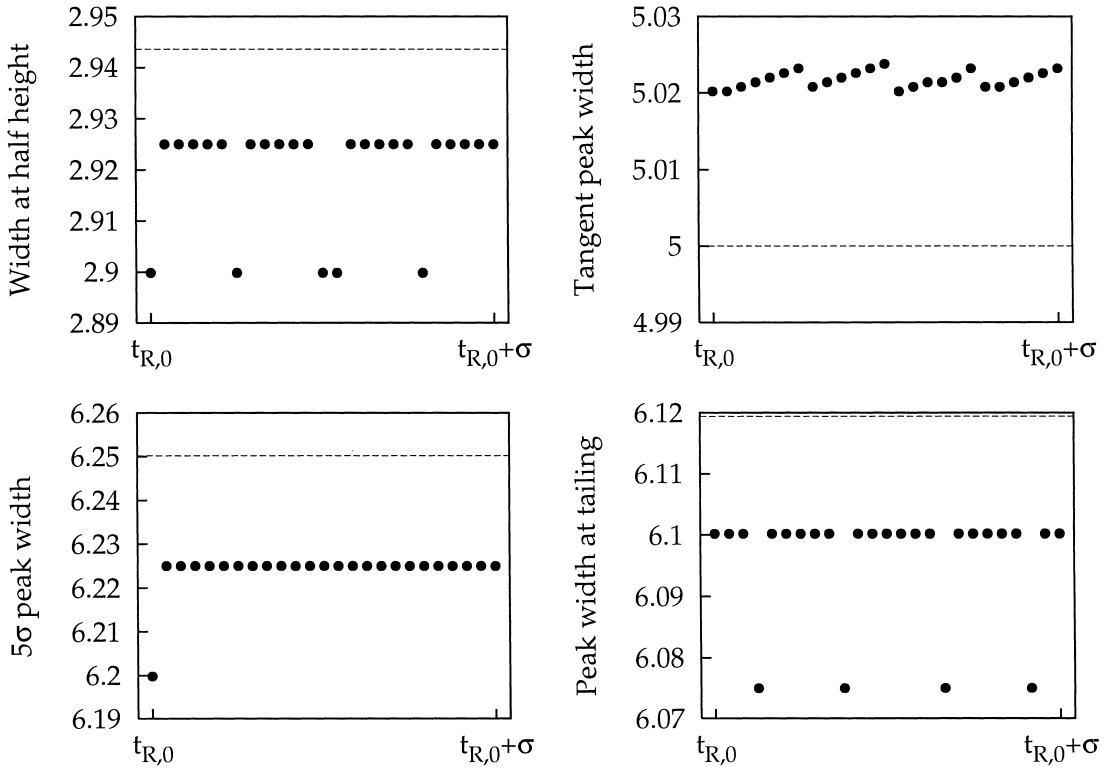

Fig. 2. Peak widths measured by four different methods when shifting the peak location.

integration of the signal and for the calculation of the moments.

4.3. Effect of noise on the accuracy and precision of the parameters

In the next series of calculations, we tested the effect of noise on the accuracy and the precision of the different peak parameters for symmetrical and asymmetrical peaks. For the sake of simplicity, we selected only one EMG and one Langmuir peak for this comparison, i.e. we did not change the degree of asymmetry of the profile. The tailing factor was 1.3 for the two asymmetrical profiles. The chromatograms were selected so that the retention time and the peak width are similar for all three models. The relative random and systematic errors observed are reported in Figs. 3–7 for the peak areas, the peak heights, the retention times, the peak widths, and the plate numbers, respectively.

These figures show that the relative standard

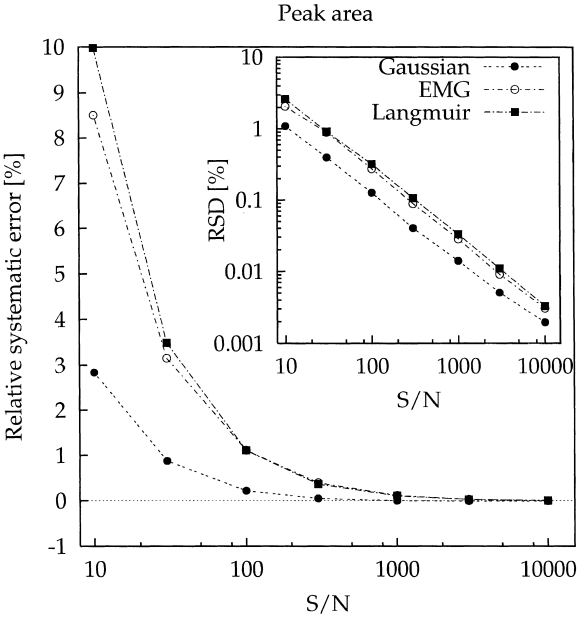

Fig. 3. Accuracy and precision of the peak area determination.

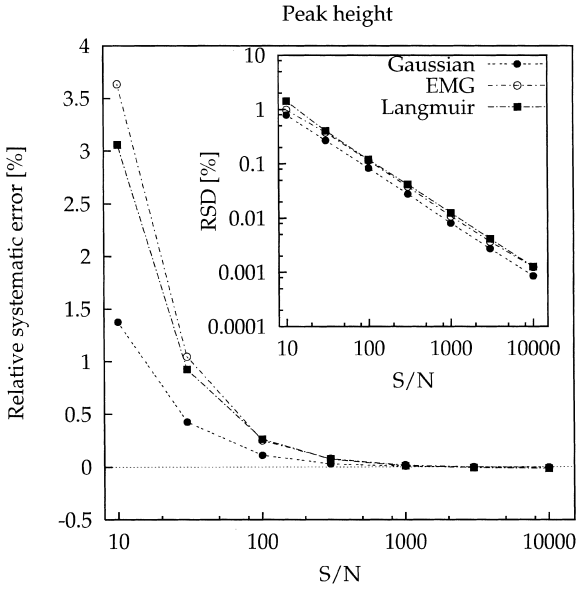

Fig. 4. Accuracy and precision of the peak height determination.

deviations of all the parameters investigated decrease linearly with decreasing signal-to-noise-ratio on a log–log plot. Both the accuracy and the precision of the peak area (Fig. 3) and the peak height (Fig. 4) determinations are best for symmetrical peaks. They are both very similar for the two asymmetrical peaks, regardless of the type of asymmetry. The precision of both parameters varies from 0.001% to about 1–2% when the signal-to-noise ratio decreases from 10 000 to 10. The accuracy of the area determination is better than 1% and that of the peak height determination better than 0.2% when the signal-to-noise ratio exceeds 100.

The accuracy of the retention time (see Fig. 5) is excellent and fairly insensitive to the baseline noise. Even for unsymmetrical peaks, the systematic error is less than 0.005% for signal-to-noise ratio in excess of 10. The precision is better than 0.1%, even when the noise level is high ($S/N=10$).

The accuracy and the precision of the peak width depend strongly on how the peak width is determined. The peak width measured at half height (see Fig. 6a) is the least sensitive to noise but its accuracy is never better than 0.3%. The peak width determined from the tangents (Fig. 6b) shows similar properties regarding both accuracy and precision. As expected, when the peak width is measured close to the baseline, it is greatly affected by noise. Therefore, the accuracy of the peak width measurement at either 4.39 (Fig. 6c) or 5% (Fig. 6d) of the peak height is not acceptable when the signal-to-noise ratio is below 100. Even at higher signal-to-noise ratios, the precision of these latter two peak widths is worse than the precision of the width determined by the tangent method. This phenomenon is most probably due to the effect of baseline fluctuation on the width close to the baseline.

In a similar manner, both the accuracy and the precision of the number of theoretical plates are worst when the plate numbers are determined on the basis of the 5σ peak width from noisy chromatograms (Fig. 7b). From noisy chromatograms the plate numbers can be determined with a slightly better accuracy but a still worse precision by means of the moments (Fig. 7d). Finally, for noisy chromatograms, both the accuracy and the precision are the best when the plate numbers are determined from the width at half height (Fig. 7a) or the tangents (Fig. 7c). At high signal-to-noise ratios, however, the moments-based calculation gives the worse precision (about 0.1%) while the accuracy is being very good.

The result obtained for the precision and accuracy of the tailing factor are plotted in Fig. 8 for the two

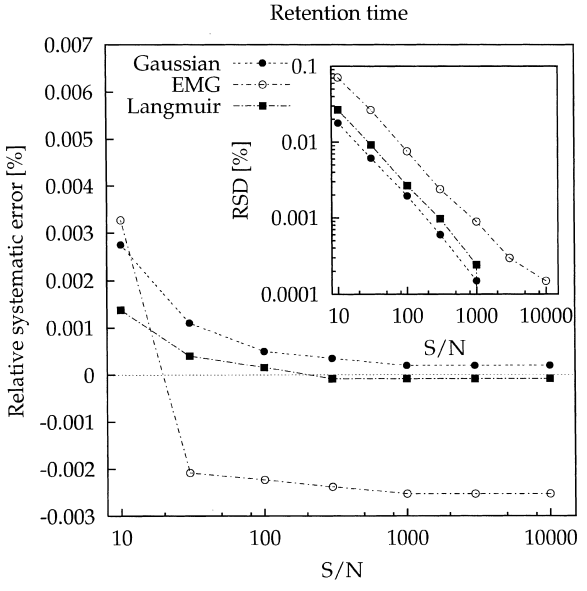

Fig. 5. Accuracy and precision of the retention time determination.

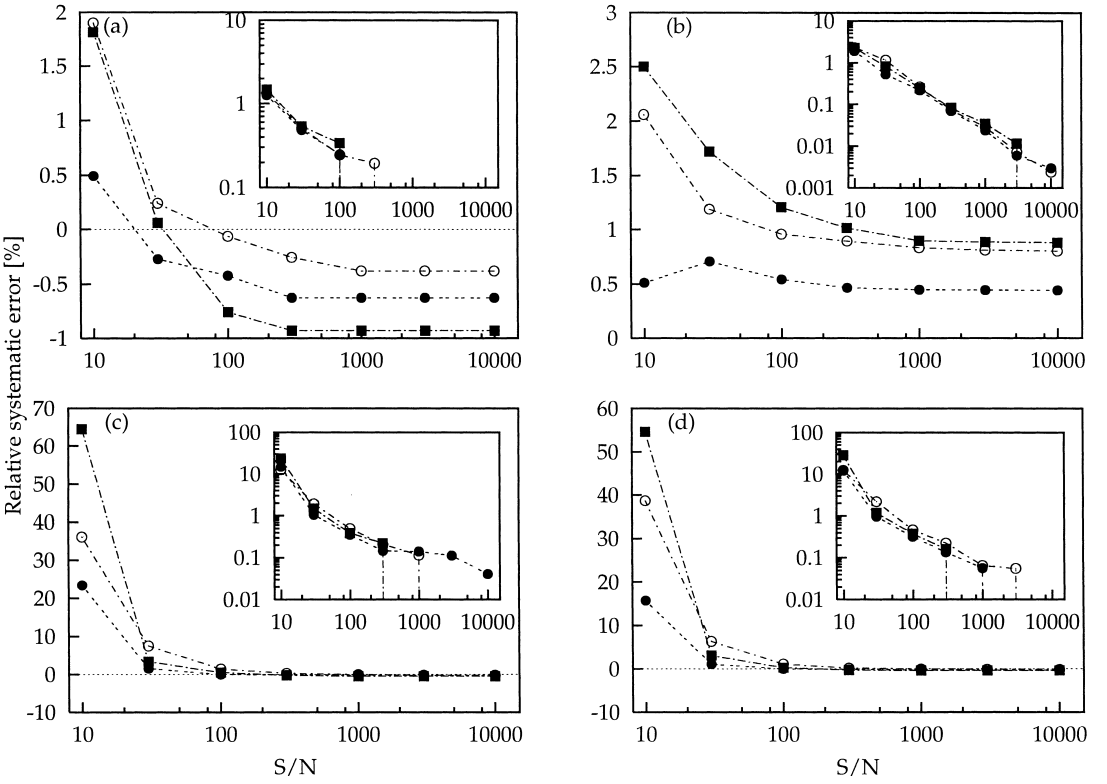

Fig. 6. Accuracy and precision of the peak width determination (a) by measuring it at half height, (b) by drawing tangents to the inflection points, (c) by measuring it at 4.39% of the peak height (5σ width), and (d) at 5% of the peak height.

asymmetrical models. Again, the results are nearly independent of the peak shape model used, although, at high signal-to-noise ratios, both the precision and the accuracy are slightly better for the Langmuir model.

4.4. Effect of peak tailing on the accuracy and precision of the parameters

In order to analyze the effect of peak tailing, peaks of increasing degree of asymmetry were generated by both the EMG and the Langmuir model. For these calculations, the signal-to-noise ratio was fixed at 300. This value was chosen because, from previous calculations (see earlier), this value was found to allow relatively small systematic and random errors. This noise level is barely detectable by looking at the chromatograms but still has a significant effect on the precision and accuracy of the estimated parameters. For both peak shape models, the asymmetry was increased up to a USP tailing factor of 3.3. The most asymmetrical Langmuir and EMG peaks that were analyzed are plotted in Fig. 9, as taken from the ChemStation report. The circles in Fig. 9 indicate the inflection points, the sloping lines are the tangents drawn to the inflection points, and the horizontal lines indicate the width at half height, at 5, and at 4.39% height, the last two barely distinguishable.

The numerical results obtained are summarized in Tables 2 and 3. As a reference, Table 1 contains the values of these same parameters but obtained for symmetrical Gaussian peaks. It can be observed that the two asymmetrical models behave in a similar manner, the ranges of the accuracy and the precision reported in Tables 2 and 3 are similar. The sole exception is the parameters that are based on the position of the inflection tangents. The software determines the inflection points and the slopes of the tangents with an exceptionally large error in the case of strongly tailing Langmuir peaks. The more

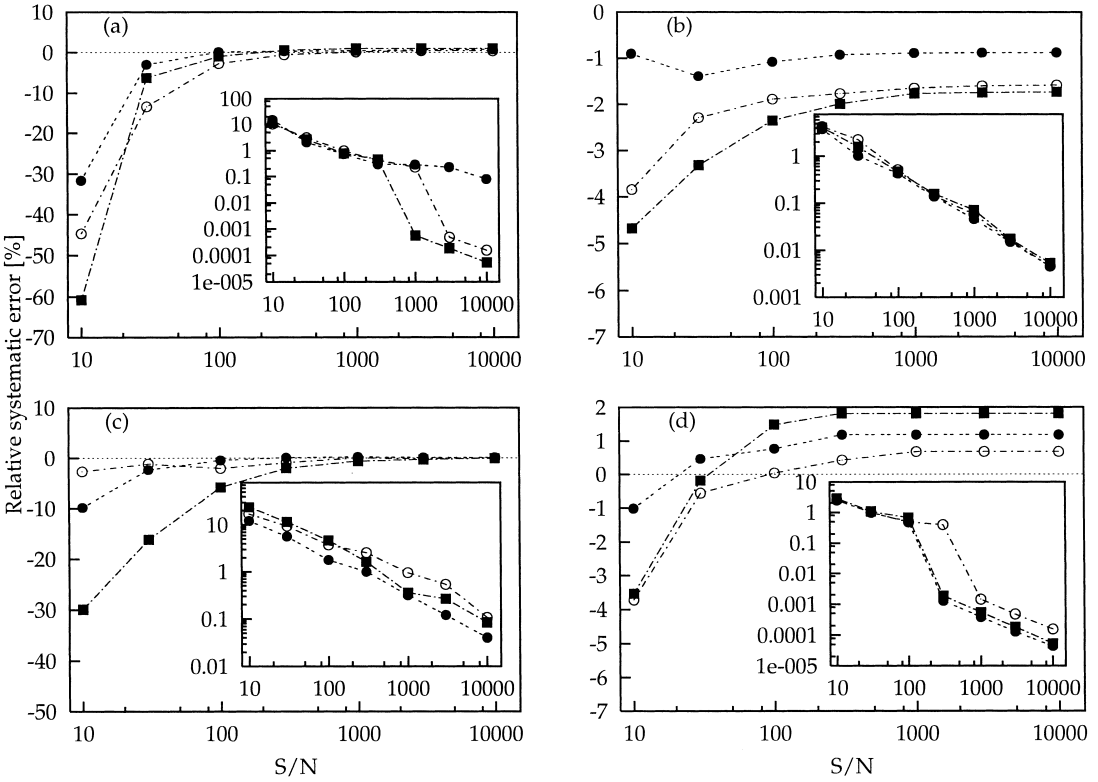

Fig. 7. Accuracy and precision of the number of theoretical plates as determined from the (a) peak width at half height, (b) 5σ width of the peak, (c) the tangent peak width, (d) the statistical moments of the peak.

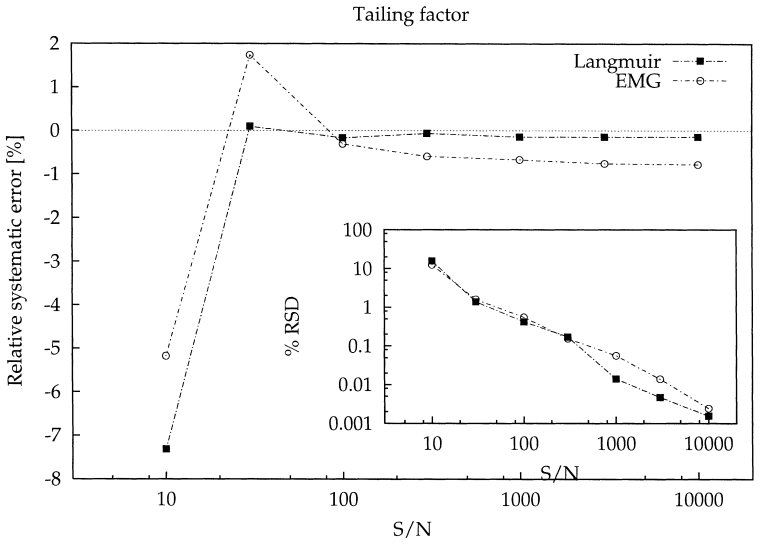

Fig. 8. Accuracy and precision of the tailing factor determination.

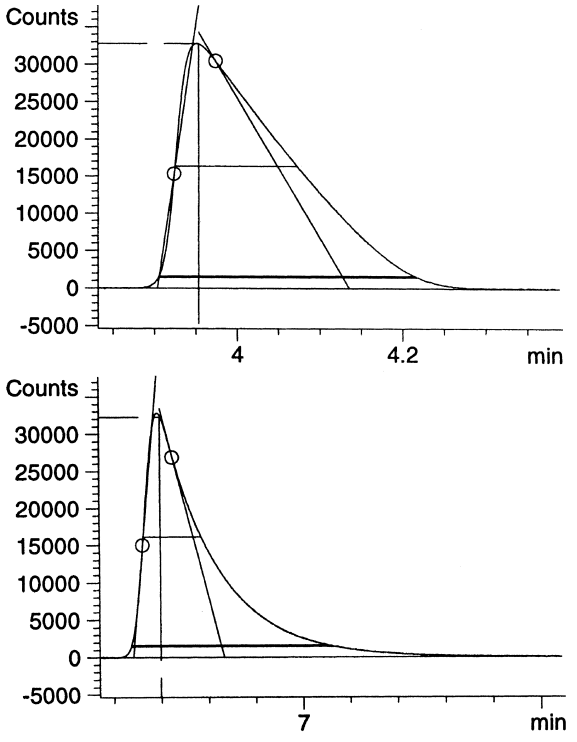

Fig. 9. Asymmetrical Langmuir (upper part) and EMG (lower part) peaks at a tailing factor of 3.3.

asymmetrical the peak, the larger the error. This is illustrated in the upper part of Fig. 9, where both the inflection point and the tangent are misplaced, particularly on the descending part of the peak.

In general, a comparison of the two tables shows that both precision and accuracy worsen with increasing degree of peak asymmetry. For most parameters, the corresponding increase in the errors made is as large as several orders of magnitude.

Table 1
Summary of the precision and accuracy achieved with processing Gaussian peaks at $S/N = 300$

	RSD (%)	Δ (%)
t_R	0.00063	0.00035
A	0.04	0.05
h_0	0.028	0.079
Width (half height)	0.0	0.63
Width (tangent)	0.00023	0.46
Width (5σ)	0.00061	0.14
Width (5%)	0.00055	0.14
N (5σ)	0.3	0.29
N (tangent)	0.14	0.92
N (statistic)	1.0	0.08
N (half height)	0.0013	1.18
Tailing factor	0.16	0.01

Table 2
Summary of the precision and accuracy achieved with processing EMG peaks at $S/N = 300$. The USP tailing factor varies between 1.1 and 3.3

	RSD (%)	Δ (%)
t_R	0.00025–0.0012	0.0003–0.0035
A	0.052–0.11	0.14–0.20
h_0	0.022–0.031	0.0096–0.42
Width (half height)	0.063–0.20	0.15–0.65
Width (tangent)	0.077–0.099	0.25–1.3
Width (5σ)	0.081–0.27	0.0035–0.20
Width (5%)	0.11–0.26	0.0017–0.15
N (5σ)	0.28–0.55	0.0055–0.47
N (tangent)	0.14–0.23	0.43–2.5
N (statistic)	1.5–4.8	0.017–2.4
N (half height)	0.13–0.37	1.18
Tailing factor	0.12–0.53	0.17–4.1

5. Conclusions

The most important conclusion of this study is that the contribution of the random and systematic errors originating from the data analysis procedure is generally far smaller than the experimental or instrumental contributions arising from the factors that affect the repeatability of chromatographic measurements. Yet, in the case of the particular software

Table 3
Summary of the precision and accuracy achieved with processing Langmuir peaks at $S/N = 300$. The USP tailing factor varies between 1.1 and 3.3

	RSD (%)	Δ (%)
t_R	0.00059–0.00080	0.0068–0.081
A	0.042–0.11	0.16–0.37
h_0	0.029–0.12	0.025–0.38
Width (half height)	0.11–0.27	0.058–0.84
Width (tangent)	0.080–1.69	0.55–24.0
Width (5σ)	0.092–0.22	0.082–0.38
Width (5%)	0.10–0.19	0.072–0.32
N (5σ)	0.18–0.45	0.30–2.1
N (tangent)	0.16–3.54	1.60–73.0
N (statistic)	0.58–1.64	0.82–2.0
N (half height)	0.0018–0.54	0.054–1.8
Tailing factor	0.11–0.29	0.065–6.0

investigated, we can write a short wish list including three items that should be enhanced. The systematic difference between the reported peak area and the 0th moment is disturbing. The peak width determination should be improved by using a proper subroutine that would fit a proper nonlinear function (parabolic or Gaussian) through several points of the acquired peak profile. The determination of the inflection points and the slope of the tangents should be reconsidered as it completely fails for some types of strongly tailing peaks. Otherwise, the accuracy and the precision of the calculated parameters are outstanding.

Acknowledgements

This work was supported in part by NATO Linkage Grant OUTR.LG971480. AF acknowledges the financial support of the Hungarian National Eötvös Foundation. We acknowledge the help of James Crabtree (Agilent Technologies, Fullerton, CA, USA) in the use of the file conversion utility.

References

[1] M. Kele, G. Guiochon, J. Chromatogr. A 830 (1999) 41.
[2] M. Kele, G. Guiochon, J. Chromatogr. A 830 (1999) 55.
[3] M. Kele, G. Guiochon, J. Chromatogr. A 855 (1999) 423.
[4] M. Kele, G. Guiochon, J. Chromatogr. A 869 (2000) 181.
[5] N. Dyson, Int. Lab. 22 (1992) 38.
[6] H. Engelhardt, C. Siffrin, Chromatographia 45 (1997) 35.
[7] T. Faller, H. Engelhardt, J. Chromatogr. A 853 (1999) 83.
[8] M. Goedert, L. Jacob, G. Guiochon, in: R. Stock (Ed.), Gas Chromatography 1970, Institute of Petroleum, London, UK, 1971, p. 160.
[9] M. Goedert, G. Guiochon, J. Chromatogr. Sci. 11 (1973) 326.
[10] H.T. Lub, H.C. Smit, H. Poppe, J. Chromatogr. 149 (1978) 721.
[11] A. Felinger, E. Vigh, A. Gelencsér, J. Chromatogr. A 839 (1999) 129.
[12] Y. Hayashi, R. Matsuda, Anal. Chem. 66 (1994) 2874.
[13] G. Guiochon, S.G. Shirazi, A. Katti, Fundamentals of Preparative and Nonlinear Chromatography, Academic Press, Boston, MA, 1994.
[14] A. Felinger, Data Analysis and Signal Processing in Chromatography, Elsevier, Amsterdam, 1998.
[15] K. Shoikhet, H. Engelhardt, Chromatographia 38 (1994) 421.
[16] S.P. Cram, S. Chesler, Anal. Chem. 43 (1971) 1922.
[17] M. Goedert, G. Guiochon, Chromatographia 6 (1973) 39.
[18] Understanding Your Chemstation, 5th ed, Hewlett-Packard Company, 1998.
[19] N. Dyson, J. Chromatogr. A 842 (1999) 321.